LOAD SHARING METHODS FOR INVERTER-BASED SYSTEMS IN ISLANDED MICROGRIDS – A REVIEW

Augustine M. Egwebe, Meghdad Fazeli, Petar Igic, Paul Holland

Electronic System Design Center at College of Engineering, Swansea University, Wales

Abstract. *This paper explores and discusses various design considerations for inverter-based systems. Different load sharing techniques are presented for the integration of renewable energy sources within islanded microgrids. In off-grid connection, renewable energy sources are often configured to share power based on their rated capacity. This paper explores both conventional and dynamic load sharing interaction between distributed generation units, both in an inductive (high voltage) and resistive (low voltage) networks. Load sharing based on the proper design of virtual impedance is also reviewed.*

Key words: *distributed generation, microgrids, droop control, virtual impedance, photovoltaic, renewable sources.*

1. INTRODUCTION

The need for clean and reliable energy generation has propelled global activity in various spheres of human endeavor to develop alternative sources of energy. The provision of affordable, reliable and sustainable access to energy in different forms remains one of the key challenges of economic and social development especially in developing countries [1, 2]. While it may be practically impossible to eliminate conventional nuclear and fossil fueled steam turbines, renewable energy sources (RES) offer huge prospects to ease the ever-increasing demand burden on large, centralized conventional power systems. Vast reduction of greenhouse gases emission can also be achieved via RES integration with the existing electricity grid networks [3].

Distributed generation is a term commonly used to describe small-scale and modular power generation sources that are located close to the distribution network rather than large power stations connected to the high voltage transmission network [4, 5]. Distributed generators (DG) includes small-scale fossil and renewable energy generation technologies including wind, photovoltaic, micro-hydro-turbines, biogas, geothermal, tidal, steam turbines with supplementary storage devices like fuel cells and batteries. DG therefore serves as a contrast to conventional large power stations that use a small number of large-scale, frequency controlled generators; it offers enhanced and improved power quality,

enhanced system security, mitigates against issues like blackout and gives better control over the cost of energy [6]. With distributed generation, consumers now have some scales of flexibility on their energy utilization [7].

Increased penetration of green renewable energy requires high-level engineering prowess in maintaining and improving the technologies that make them effective, durable and sustainable [8]. The integration of RES with the existing power network mainly involves the strategies and schemes employed via the use of technologies, processes, and advanced control protocols to balance the production and demand of electrical energy within the network. These control schemes enhance the reliability of energy supply irrespective of the intermittent nature of the renewable source (i.e. fluctuating sunshine or wind profile). They include strategies for the optimal harnessing of the available renewable power, effective energy management, power/voltage device control, intelligent control of energy transformation, islanding detection, and line faults management [7-9]. To balance generated energy with demand in modern microgrids, various renewable sources and converters are often interconnected for load sharing and complimentary energy support. Renewable power generation units are also often supplemented with dispatchable resources such as energy storage systems and local auxiliary generators; where the absence of such resources can result in the malfunctioning of the inverter-based sources (IVBS) [10].

An intermediate solution to some of the problems with the integration of DG with the existing power network is the concept of the microgrid shown in Fig. 1 - an electrical distribution system using distributed energy resources such as generators, storage devices and controllable loads which are coordinated, when connected to the main power network or operated in islanded mode [9, 10]. In grid-connected mode, control measures are relatively easy to be implemented since the utility grid regulates voltage and frequency for loads within the microgrid; whereas in islanded mode voltage and frequency must be actively controlled for the continuous and stable performance of the network [11-13]. The microgrid, when operated in islanded mode, must be able to integrate and coordinates several energy resources with appropriate voltage-frequency control strategies. The electrical power generated from DGs must be well regulated to suit sensitive non-linear loads within the distribution level (i.e. computers, motor drives, battery chargers), without causing unregulated constraint on the generator. The control measures in DGs also aim to offer greater power quality control and low voltage ride through required for eliminating transient stability issues [14, 15]. Additionally, microgrids help to reduce congestion on the utility grid, serves as uninterrupted supply for critical loads, encourage the localized generation of power on the consumer side and offer extra support regarding voltage support, demand response as well as spinning reserve via inbuilt storage devices [16].

The hierarchical control approach employed in a microgrid allows autonomously coordinated generation output from DGs and energy storage systems while ensuring the appropriate load sharing and interaction with the National Grid (NG) [17]. In the absence of free generation capacity in the system due to each DG hitting their maximum generating capacity, the microgrid should be self-sustainable without violating sensitive network parameters like voltage and frequency [18].

A microgrid can connect and disconnect from the NG to enable it to operate in either grid-connected or islanded mode using the microgrid central switch shown in Fig. 1. A required basic characteristic of the microgrid is seamless "islanding" and "reconnection" from/to the NG. Disconnection can be as a result of grid events which include faults, voltage collapse, and blackout [8, 19]. All DGs within the microgrid must be well regulated to present peer-to-peer and plug-and-play characteristics.
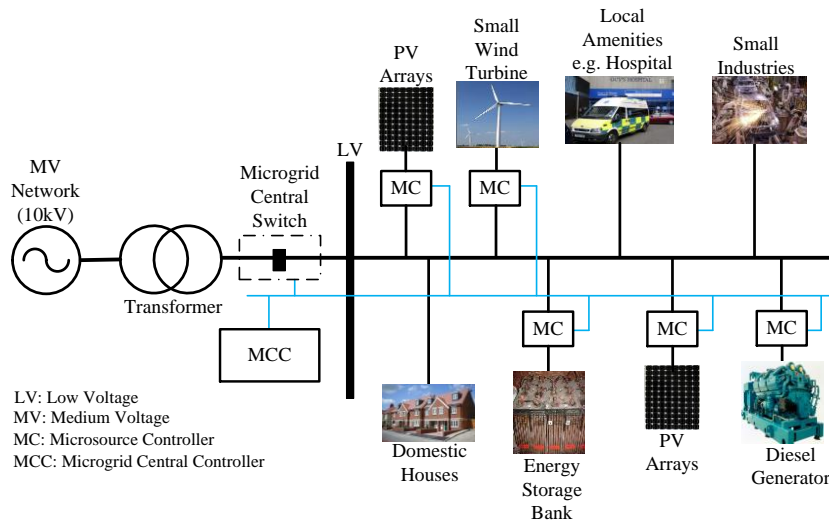
Fig. 1 An example of a microgrid network

Islanding detection of distributed generation systems, voltage regulation, protection, power quality improvement and stability of the power system network are some of the technical challenges facing DGs as they are increasingly connected to the microgrids. Accurate and intelligent controller design is thus required to ensure swift interaction with connected loads and the microgrid while ensuring system stability when disconnecting from the NG in the case of fault or disturbance [20].

In this paper, a thorough survey of the core components and techniques required for the effective integration of DGs in an islanded microgrid is presented. Control paradigms to facilitate the efficient load sharing, operation, and energy management of DGs in a microgrid is also presented.

2. INVERTER-BASED SYSTEMS

Inverter-based systems (IVBS) play a vital role in the effective integration of renewables with the microgrid at a synchronized system frequency. IVBS are commonly employed for switching DC voltages from renewable sources to AC voltages supplied to the microgrid and locally connected loads [19, 21]. Monitoring and control functionality are essential requirements for the power electronics interface used in IVBS so as to ensure the protection of the DG system and as well as meet the connection specifications of the NG [19]. Active power, reactive power, voltage and frequency at the point of common connection are some of the critical monitoring parameters for these types of systems as shown in Fig. 2. Also, proper conditioning of voltage and current ensures successful control of power flow per specific power references under varying load or DG input sources. Motor drives and distributed generation systems use IVBS due to their inherent advantages of adjustable power factor, low total harmonic distortion (THD), and their high efficiency.
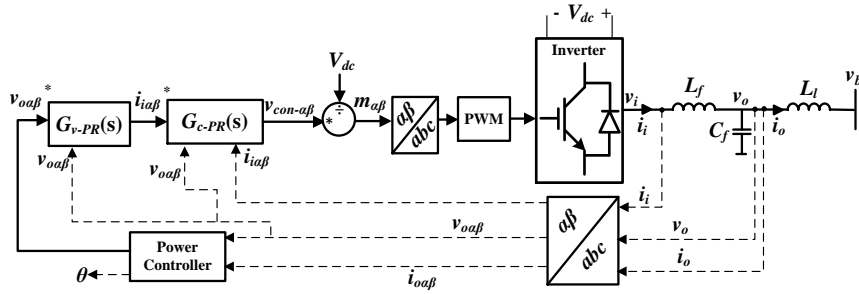
Fig. 2 Generic inverter-based system

A conventional inverter circuit consists of controllable transistorized switches, such as IGBTs with parallel diodes to provide a bypass path for transient currents as shown in Fig. 3.a. The three-phase IGBT bridge circuit operates according to the control signal (v_{con}) generated by the control algorithm of the controller as shown in Fig. 3.b. The three-phase IGBT-based inverter in Fig. 3 consists of six switching devices (Q_1 - Q_6), which are directly controlled by pulse width modulation (PWM) signals (S_1 through S_6) to be ON (closed) or OFF (open) according to a well-structured switching pattern to produce the desired output AC waveforms [23, 24].
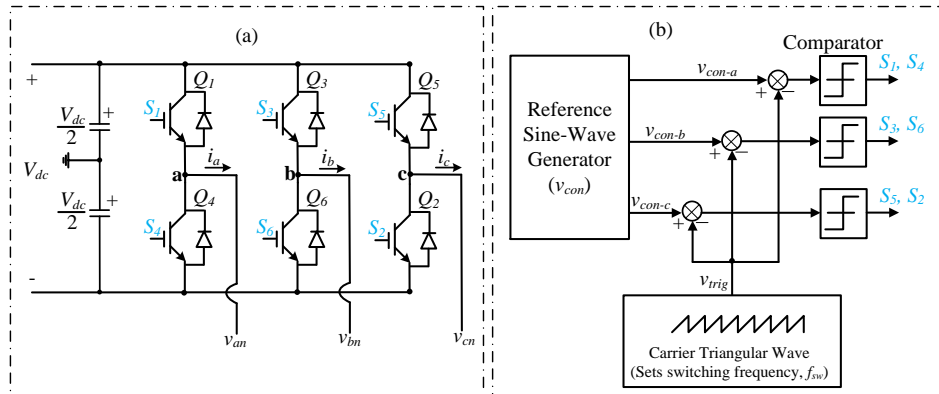

Fig. 3 (a) Three-phase bridge inverter [22]; (b) SPWM control signal generator [22]

The use of PWM switching together with closed-loop voltage and current controllers produces a sinusoidal output current in phase with the grid voltage with THD aligned to grid regulations. Conventional grid-mode IVBS in PV applications ensure that: (1) PV modules operate at maximum power point (MPP); (2) the injected AC current into the grid is sinusoidal, with consideration for the IEEE 547 demand standards for grid connection. These standards include issues such as power quality, islanding detection mode, grounding and harmonics. One of the challenges of switching IVBS at high frequencies (2 - 20 kHz) is the creation of high-order harmonics. THD in current and voltage can lead to low power factor, overheating of distribution system components, mechanical oscillation in generators and motors, poor performance of communication equipment, and unpredictable behavior of

security protection systems [22, 23, 25]. The low-pass filter connected to the output of the inverter helps to prevent the injection of high-frequency harmonics into the AC bus [23, 25]. Line frequency transformers are used for galvanic isolation when interfacing the microgrid with the NG as shown in Fig. 1.

Sinusoidal pulse width modulation (SPWM) is the simplest continuous carrier-based PWM method for generating pulses, and for switching inverter-based devices with a fundamental frequency of 50 or 60 Hz. The main objectives of any modulation scheme are: (1) lower switching losses, (2) reduced THD of output current, (3) minimize computational switching time, (4) better DC bus utilization, and (5) easy digital implementation [26].

In the SPWM-based system in Fig. 2, the three-phase fundamental components of the AC output voltage of the inverter are given by (1) [27-31].

$$
\begin{aligned}
v_{i-a} &= 0.5 m_a V_{dc} \cos(\omega_0 t) \\
v_{i-b} &= 0.5 m_b V_{dc} \cos(\omega_0 t - 120^0) \\
v_{i-c} &= 0.5 m_c V_{dc} \cos(\omega_0 t + 120^0)
\end{aligned}
\tag{1}
$$

where m_a, m_b, m_c = modulation index per phase; V_{dc} = DC link voltage; and ω_0 = fundamental angular frequency of the system.

By using the vector-control approach, (1) can be represented as $\alpha\beta$-components hence offering better tracking performance at steady state for the proportional-resonant (PR) controller as shown in (2).

$$
\begin{aligned}
v_{i-\alpha} &= 0.5 m_\alpha V_{dc} \\
v_{i-\beta} &= 0.5 m_\beta V_{dc}
\end{aligned}
\tag{2}
$$

The magnitude of the AC output voltage of the DG in (2) is provided in (3)

$$
\left| v_{i-\alpha\beta} \right| = 0.5 V_{dc} \sqrt{m_\alpha{}^2 + m_\beta{}^2} = 0.5 m V_{dc}
\tag{3}
$$

In (3), the fundamental component of the AC output voltage is thus controlled by controlling the inverter amplitude modulating index m. Where m is defined as the ratio of the amplitude of the modulated signal to that of the carrier signal. The inverter switching process works well for $0 < m < 1$ to prevent unwanted harmonic distortion [23, 32, 33].

The DC link voltage V_{dc} of the inverter-based source must satisfy (3) to avoid PWM over modulation and to ensure the stable operation of the DG in a microgrid. However, when there is a reduction in renewable energy resource level (i.e. wind or solar irradiance level) hence decreasing V_{dc}, m must increase to maintain $v_{i-\alpha\beta}$ in (3). At $m = 1$; a fixed $v_{i-\alpha\beta}$ depends solely on V_{dc}. Therefore, when designing the IVBS, consideration for the minimum DC link voltage to satisfy (3) must be ensured.

The diagrammatic description of the closed-loop control scheme of each inverter-based DG in an islanded microgrid is shown in Fig. 2. The direct Proportional-Resonant (PR) control approach can be used to simplify Fig. 2 as shown in the block diagram representation in Fig. 4.
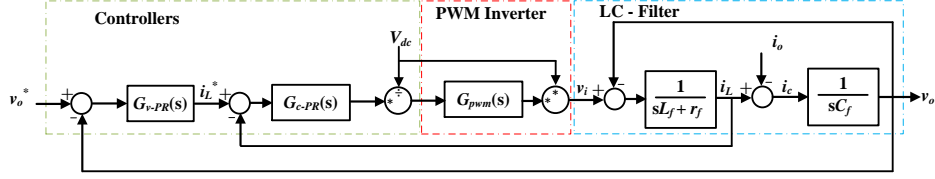
Fig. 4 Block diagram of the closed-loop inverter-based source [20, 34]

In the closed-loop DG model in Fig. 4, an outer voltage loop $G_{v\text{-}PR}$ is used to control the output voltage of the inverter. The main control objective of $G_{v\text{-}PR}$ is to maintain a clean and balanced DG voltage as close as possible to the given sinusoidal reference voltage so that the THD of the output voltage is minimized. The voltage reference is compared with the measured voltage in $\alpha\beta$-frame to produce an error signal. The error signal is fed into a PR compensator, which in turn generates the current reference signal for the inner current loop. Similarly, in the inner current controller G_{c_PR} in Fig. 4, the reference current from the outer voltage loop is compared with the measured output current. The error signal is fed into a PR controller to generate the reference signal for the PWM generator. The controlled output wave from the current controller is transformed back to the abc-frame using the abc/$\alpha\beta$-coordinate transformation principle, to generate the reference control signal for the inverter switching devices. The bandwidth of the inner current controller is usually designed to be much faster than the outer voltage loop to achieve a fast dynamic response. In general, the voltage and current controllers are designed to provide nearly perfect sinusoidal output voltage waveforms at a nominal switching frequency and to offer good damping for the output filter of the inverter and the rejection of high-frequency disturbances.
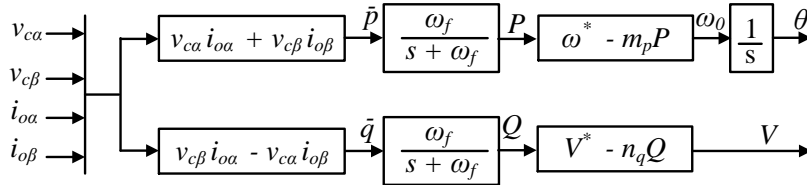

Fig. 5 Droop controlled power sharing for islanded DG [30]

The dynamics of the control scheme depends mainly on the bandwidth of the *PQ* controller shown in Fig. 4, since the bandwidth of the current and voltage controller, are designed to be much higher than that of the *PQ* controller [25]. The power controller block is used for accurate sharing of *P* and *Q* according to the droop characteristics as shown in Fig. 5 [10]. The low-pass filter with cutoff frequency w_f is used to extract the average powers as shown in Fig. 5.

The non-ideal PR controller adopted in this paper can overcome two well-known drawbacks of conventional PI controller: (1) the inability to track a sinusoidal reference with zero steady-error, (2) poor disturbance rejection capability. This is due to the PR controller infinite gain at the fundamental frequency [35], thus reducing steady state error to zero.

Equation (4) shows the transfer function of the adopted practical non-ideal PR controller to achieve finite gain at the AC line frequency.

$$G_{PR}(s) = K_p + \frac{2K_i\omega_c s}{s^2 + 2K_i\omega_c s + \omega_o^2} \tag{4}$$
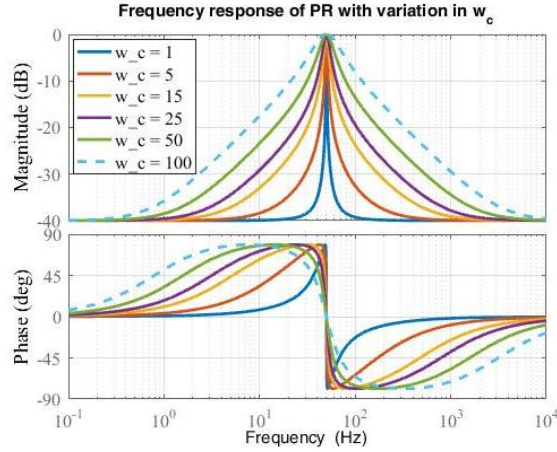

Fig. 6 Frequency response of a PR controller for $K_p = 0.01$,
$K_i = 1$ and $\omega_c = 1, 5, 15, 25, 50, 100$ rad/s

The frequency response of (4) shows a wider bandwidth around the 50 Hz resonant frequency which helps to minimize any slight frequency variation due to load disturbance. The PR controller's bandwidth can be varied with the damping factor ω_c as shown in Fig. 6. It can be seen that ω_c has an effect on both the magnitude and phase of the controller. When choosing ω_c, there has to be a compromise between the reduction of sensitivity and steady state error.

2.1. Current controller design

The design objective of the current controller is to have a high loop bandwidth with sufficient stability margins. It is noted from control laws that systems with greater gain margins can withstand greater changes in the systems parameters before becoming unstable in the closed loop response. When designing via frequency response analysis, the goal is to predict the closed-loop behavior from the open-loop response of the current control loop shown in Fig. 4. The closed-loop transfer function of the current loop when the output current is assumed as disturbance is given in (5) [36]. Feedforward terms are added to the current loop in order to decouple the αβ components of the output voltage [37].

$$G_c(s) = \frac{i_L}{i_L^*} = \frac{G_{c-PR}(s)G_{pwm}(s)G_{Lf}(s)}{1 + G_{c-PR}(s)G_{pwm}(s)G_{Lf}(s)} \tag{5}$$

where G_{c-PR} is the PR current controller; G_{Lf} is the transfer function of the LC filter respectively; $G_{pwm}(s) = 1 / (1+1.5T_s s)$ represents the PWM and computational delay with

respect to the sampling period T_s. By setting ω_c in (4) equal to 10 rad/s, (5) can be tuned for a closed-loop bandwidth of 1 kHz to give K_p and K_i of 12.5Ω and 250Ω respectively. Note that the bandwidth of (5) is usually selected as one-tenth of the switching frequency.

2.2. Voltage controller design

The voltage controller is also based on the PR structure discussed in (4), where a generalized integrator is used to achieve a zero steady-state error. The closed-loop dynamic behavior of the DG in Fig. 4 is approximated as an equivalent Thevenin equation as given in (6):

$$\left.\begin{aligned} v_o &= \frac{G_{pwm}(s)G_{c-PR}(s)G_{v-PR}(s)}{s^2 A_x + sB_x + C_x} v_o^* - \frac{sL_f + r_f + G_{pwm}(s)G_{c-PR}(s)}{s^2 A_x + sB_x + C_x} i_o \\ v_o &= G_o(s)v_o^* - Z_o(s)i_o \end{aligned}\right\} \qquad (6)$$

where $A_x = L_f C_f$; $B_x = (r_f + G_{pwm}(s)G_{c-PR}(s))C_f$; $C_x = G_{pwm}(s)G_{c-PR}(s)G_{v-PR}(s)$; $G_{v-PR}(s)$ is the PR capacitor voltage controller; r_f is the parasitic resistance of the filter inductor; $G_o(s)$ is the control closed-loop system transfer function; $Z_o(s)$ is the output impedance.

Fig. 7 shows the open-loop frequency response of the DG's voltage loop when the output current is assumed as disturbance, the positive high gain margin (46.4 dB) and phase margin (79.3 degrees) both confirm the stability of the overall system. The bandwidth of the voltage controller is tuned to be about one-fifth of the bandwidth of the current controller as shown in the closed loop frequency response in Fig. 8, to give K_p and K_i values of 0.5Ω and 7 Ω respectively.
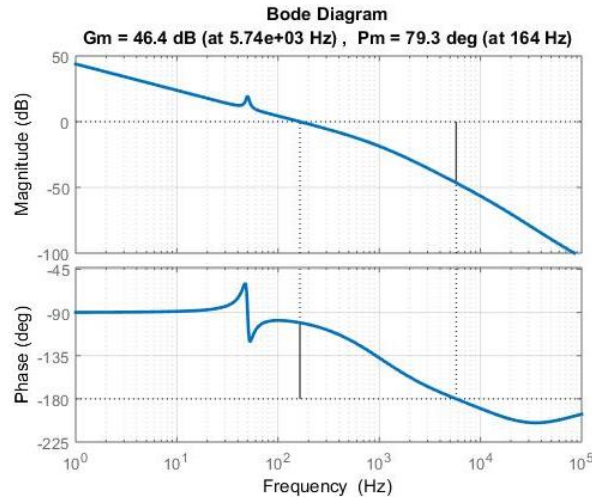

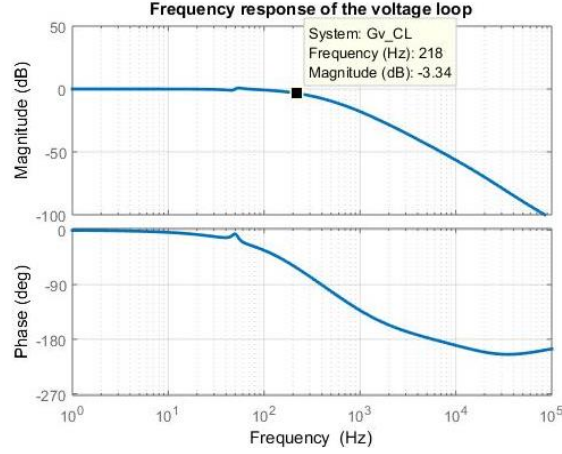**Fig. 7** Open-loop frequency response of the DG voltage loop

Fig. 8 Closed-loop frequency response of the DG voltage loop

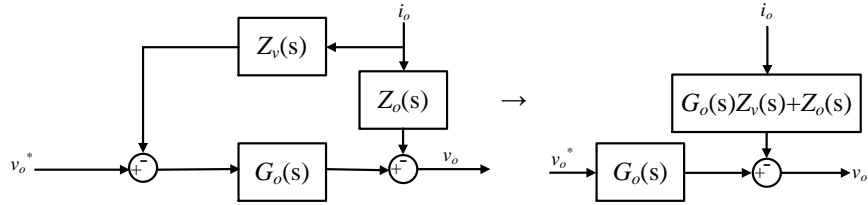### 2.3. Virtual impedance design for *P* and *Q* decoupling

Fig. 9 Block diagram representation of virtual impedance loop

In order to ensure a stable output impedance of the DG, the output DG voltage is dropped proportionally with the output current as shown in Fig. 9 and explained in (7):

$$v_o = G_o(s)v_o^* - (G_o(s)Z_v(s) + Z_o(s))i_o \qquad (7)$$

The output impedance of the inverter is re-designed to mitigate the influence of control parameters and line impedance on the power-sharing accuracy around the fundamental frequency as shown in Fig. 9, to share the power precisely between the distributed IVBS [34]. References [21, 34, 38, 39] proposes a design scheme to eliminate the impact of DG output impedance on the overall system dynamics; hence the virtual impedance loop was implemented for power decoupling and restraining of circulating current between DGs.

A performance comparison of virtual impedance techniques used in droop-controlled islanded microgrids was presented in [40, 41]. It was noted that the virtual inductive loop helps to improve the output impedance of the inverters such that it becomes predominantly inductive thereby improving the power-sharing accuracy of the droop control algorithm. Similarly, a virtual resistive loop increases the output impedance of the inverters such that it becomes more resistive. The overall effect of impedance mismatches is also reduced by

the virtual resistance loop thereby improving the current sharing. A virtual resistance allows sharing of linear and nonlinear loads in microgrid applications without introducing additional losses in the network and improves the stability of the microgrid [41].

According to Fig. 10, the magnitude of the IVBS output impedance at the fundamental frequency is approximately zero. This shows the effectiveness of the designed control parameter of the voltage and current loop. Hence, the output impedance of the IVBS is designed to be equal to the virtual impedance around the fundamental frequency as shown in Fig. 10. Fig. 10 also illustrates the effect of the virtual inductance on the overall output impedance of the IVBS. As can be seen, the overall output impedance become more inductive as the virtual inductance increases.
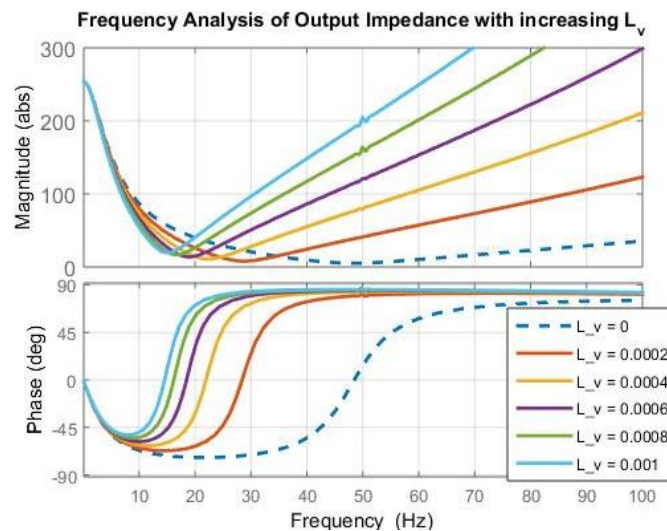

Fig. 10 Output impedance frequency response of the IVBS with varying virtual inductance

3. CONVENTIONAL LOAD SHARING SCHEMES IN AN ISLANDED MICROGRID

Load sharing without communication between the parallel DGs is the most favored option in an autonomous microgrid as the network can be complex and can span over a large geographical area [19, 42]. Numerous literature has studied and presented the droop scheme so that parallel DGs can be locally controlled to deliver required active and reactive power to the microgrid network. By adopting the droop scheme, two local independent network quantities (voltage and frequency) are controlled to regulate active and reactive power with consideration for the allowable frequency and voltage deviation within the microgrid. The small-signal stability analysis of the droop scheme has also been explored in the various literature [19, 30, 43]. One major concern with the droop scheme is its sensitivity to the imbalance in the system's closed-loop output impedance and line impedance, which can lead to poor coupling between the active and reactive power [21, 42].

The complex power delivered to the common bus in Fig. 2 can be expressed as shown in (8).

$$S = P + jQ \tag{8}$$

$$\left.\begin{aligned} P &= \frac{V_o V_b}{Z} \cos(\theta - \phi) - \frac{V_b^2}{Z} \cos\theta \\ Q &= \frac{V_o V_b}{Z} \sin(\theta - \phi) - \frac{V_b^2}{Z} \sin\theta \end{aligned}\right\} \tag{9}$$

where P and Q are the active and reactive power delivered by the DG; V_o is the AC output voltage of the DG; V_b is the bus voltage; Z is the magnitude of the output impedance, and Θ is the phase angle of the output impedance.

3.1. Active power-frequency droop scheme

Conventionally, the output impedance is considered to be purely inductive (i.e. $Z \approx jX$), hence (9) is re-written as in (10).

$$\left.\begin{aligned} P &= \frac{V_o V_b}{X} \sin\phi \\ Q &= \frac{V_o V_b}{X} \cos\phi - \frac{V_b^2}{X} \end{aligned}\right\} \tag{10}$$

The power droop controller in Fig. 5 aims to adjust the frequency and voltage difference relative to increasing load in a stable manner. In an inductive-based microgrid, the droop equation is expressed as (11) and shown in Fig. 13.

$$\left.\begin{aligned} \omega_0 &= \omega^* - m_p(P - P^*); \phi = \omega_0 \\ V &- V_o^* - n_q(Q - Q^*) \end{aligned}\right\} \tag{11}$$

Where ω^* is the fundamental frequency; V^* is the AC reference voltage; P^* and Q^* are the reference active and reactive powers; ϕ is the power angle, P and Q are the instantaneous active and reactive power of the DG. The droop gains m_p and n_q are calculated for a given range of frequency and voltage as shown in (12)

$$m_p = \frac{\omega_{max} - \omega_{min}}{P_{rated}} ; \quad n_q = \frac{V_{max} - V_{min}}{Q_{rated}} \tag{12}$$
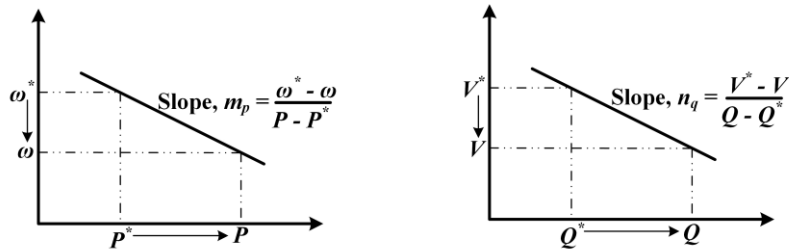

Fig. 11 Steady-state characteristic of conventional droop scheme

Equation (11) indicates that the active power of the DG is dependent on the power angle, whereas the voltage amplitude difference mainly influences the reactive power. Equation (13) shows the load distribution for N-parallel connected DGs in a microgrid when (11) is adopted.

$$m_{p1}P_1 = m_{p2}P_2 = ... = m_{pN}P_N$$
$$n_{q1}Q_1 = n_{q2}Q_2 = ... = n_{qN}Q_N$$

(13)

3.2. Active power-voltage droop scheme

It is noted in the various literature that the performance of the conventional droop control is severely affected by the resistance-to-inductance (R/X) ratio of output and the line impedance. Equation (9) is given as (14) when the output impedance of the DG is resistive (i.e. $Z \approx R$):

$$P = \frac{V_o V_b}{R}\cos\phi - \frac{V_b^2}{R}$$
$$Q = -\frac{V_o V_b}{R}\sin\phi$$

(14)

Since low voltage microgrid electrical distribution networks present a high R/X ratio, the voltage amplitude is used to control active power, while reactive power is controlled by the system frequency as shown in (15).

$$\omega_0 = \omega^* + m_p(Q - Q^*); \phi = \omega_0$$
$$V_o = V_o^* - n_q(P - P^*)$$
$$m_p = \frac{\omega_{max} - \omega_{min}}{Q_{rated}} \; ; \; n_q = \frac{V_{max} - V_{min}}{P_{rated}}$$

(15)

3.3. Virtual impedance load sharing scheme

The active and reactive power can also be well autonomously controlled using the virtual impedance scheme in (16) without any requirement for additional power controller as studied in [43]. Equation (16) ensures accurate load sharing between the DGs and compensates reactive power differences due to output voltage mismatches, or line impedance mismatches. In order to avoid the steady-state frequency deviation, a PLL is introduced. This way, the PLL adjust the phase of the inverter, and the system is controlled by a virtual resistance controlling current as in a dc electrical system. Reference [44] proposes an autonomous loading sharing scheme using the virtual resistance loop and a synchronous reference frame phase-locked loop. This scheme provides for both instantaneous current sharing and fast dynamic response of the paralleled IVBS. The relationship between the $I_{o\alpha\beta}$ and the virtual resistance R_v for N-DGs is given as (16).

$$I_{o\alpha1}R_{v1} = I_{o\alpha2}R_{v2} = ... = I_{o\alpha N}R_{vN}$$
$$I_{o\beta1}R_{v1} = I_{o\beta2}R_{v2} = ... = I_{o\beta N}R_{vN}$$

(16)

The small-signal analysis shows that the output α and β axis output currents of paralleled inverters are inversely proportional to their virtual resistances since the current

sharing performance is just influenced by the output impedance ratio instead of the output impedance value of the DGs [43].
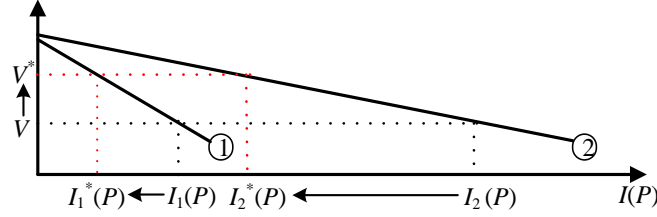

Fig. 12 Characteristics of virtual impedance droop (*V-P*)

3.4. Energy saving via dynamic load sharing

Reference [10] presented a dynamic load sharing scheme for photovoltaic (PV) inverter-based systems in an inductive microgrid, by using the PV array's current vs voltage characteristics in defining an operating range for the inverter-based source. The dynamic load sharing scheme is based on the available solar power to ensure an efficient load sharing interaction with other DGs, without the need for energy support from local connected fossil-fuelled auxiliary generator and thereby providing significant energy saving compared with conventional static droop control techniques.

In the dynamic loading scheme, the droop gains of the power controller in (11) are re-defined for dynamic load interaction between the DGs [45] as follows:

$$m_p = \frac{\Delta\omega}{P_{DC-\max}} \quad ; \quad n_q = \frac{\Delta V}{Q_{avail}} \tag{17}$$

where P_{DC-max} is the maximum available power of the PV array which is deduced from the maximum power curve in Fig. 13. Q_{avail} is the available reactive power that the DG can supply as defined in (18).

$$Q_{avail} = \sqrt{S_{rated}{}^2 - P_{DG}{}^2} \tag{18}$$

Figure 14 shows the load sharing profiles of two DGs interfaced to the islanded microgrid [10]. Fig. 14.b shows load sharing based on the conventional droop scheme in (11), where a drop in the available power of DG_2 causes similar drop in DG_1 even though it has enough available capacity. As a result, the total generation becomes less than the load, the auxiliary generator (AG) is thus triggered on to supply the shortage in supply P_{aux}. In Fig. 14.c, the load is adaptively shared based on the available PV power using (17). Thus, a drop in the available energy in DG_2 causes a proportional drop in its contribution to P_{Load}. Similarly, DG_1 dynamically compensate for this drop by supplying more power. Hence no extra power is required from the AG ($P_{aux} \approx 0$ in Fig. 14.c).
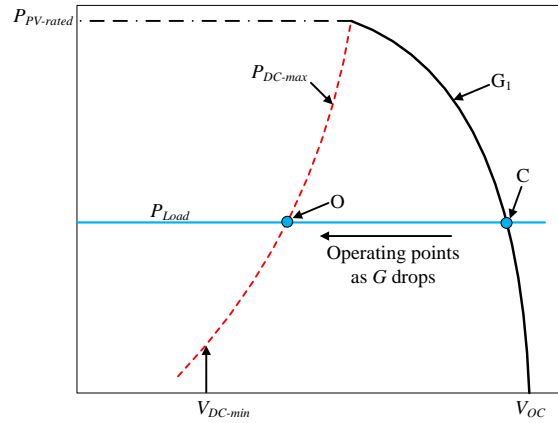
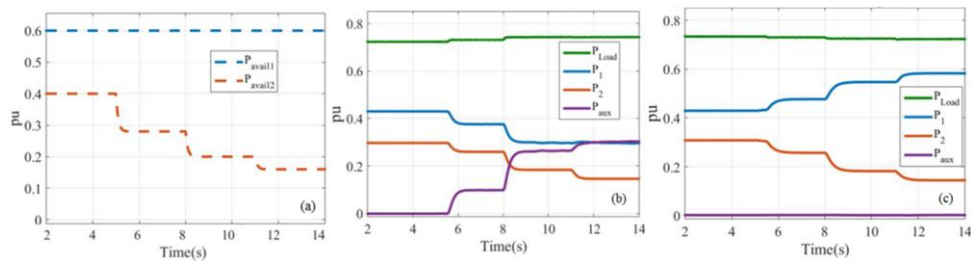**Fig. 13** Steady-state characteristic of PV operating zone

Fig. 14 Simulation results of two DG systems using droop-based load sharing scheme showing Active Power Sharing (a) available solar power in pu; (b) Static scheme: active power in pu (d) Dynamic scheme: active power in pu.

4. CONCLUSION

A thorough review of the effective integration of inverter-based systems in islanded microgrids was presented in this paper. Different control and load sharing method were discussed with respect to the output impedance of the DG, and a frequency response analysis influence of the PR controller on the performance of the DG was also presented. In the dynamic load sharing scheme presented, the droop parameters were tuned based on the available power of the DG. The dynamic load sharing scheme offers energy savings when compare to the conventional loading scheme.

REFERENCES

[1] M. Olken and A. Zomers. (2014, Jul.- Aug.) Energy for All: World Access to Electricity. *Power and Energy Society.*
[2] J. C. Vasquez, J.M. Guerrero, M. Savaghebi, J. Eloy-Garcia and R. Teodorescu, "Voltage Support Provided by a Droop-Controlled Multifunctional Inverter," *IEEE Trans. Ind. Electronics,* vol. 56, pp. 4510-4519, Oct. 2009.

[3] P. Basak, S. Chowdhury, S. Halder, S. P. Chowdhury, "A literature review on integration of distributed energy resources in the perspective of control, protection and stability of microgrid," *Renewable and Sustainable Energy Reviews,* vol. 16, pp. 5545-5556, 2012.

[4] N. Jenkins, R. Allan, P. Crossley, D. Kirshen, and G. Strbac, *Embedded Generation*. London: The Institute of Electrical Engineers, 2000.

[5] Y. Levron, J. M. Guerrero and Y. Beck, "Optimal Power Flow in Microgrids With Energy Storage," *IEEE Transactions on Power Systems,* vol. 28, pp. 3226-3234, 2013.

[6] M. Milligan, B. Frew, B. Kirby, M. Schuerger, K. Clark, D. Lew, P. Denholm, B. Zavadi, M. O'Malley, and B. Tsuchida, "Alternatives No More: Wind and Solar Power Are Mainstays of a Clean, Reliable, Affordable Grid," *IEEE Power and Energy Magazine,* vol. 13, pp. 78-87, 2015.

[7] P. K. Olulope, K. A. Folly, and G. K. Venayagamoorthy, "Modeling and simulation of hybrid distributed generation and its impact on transient stability of power system," In Proc. of the 2013 IEEE International Conference on Industrial Technology (ICIT), 2013, pp. 1757-1762.

[8] Q. Fu, A. Hamidi, A. Nasiri, V. Bhavaraju, S. B. Krstic, and P. Theisen, "The Role of Energy Storage in a Microgrid Concept: Examining the opportunities and promise of microgrids," *IEEE Electrification Magazine,* vol. 1, pp. 21-29, 2013.

[9] G. A. Jimnez-Estevez, "Energy Access Challenge: It Takes a Village," *IEEE Power and Energy Society Trans. ,* vol. 12, pp. 60-69, 2014.

[10] A. M. Egwebe, M. Fazeli, P. Igic, and P. M. Holland, "Implementation and Stability Study of Dynamic Droop in Islanded Microgrids," *IEEE Transactions on Energy Conversion,* vol. 31, pp. 821-832, 2016.

[11] J. Rocabert, G. M. S. Azevedo, A. Luna, J. M. Guerrero, J. I. Candela, and P. Rodrixguez, "Intelligent Connection Agent for Three-Phase Grid-Connected Microgrids," *IEEE Trans. Power Electronics,* vol. 26, pp. 2993-3005, Oct. 2011.

[12] J. Y. Kim, J. H. Jeon, S. K. Kim, C. Cho, J. H. Park, H. M. Kim, and K. Y. Nam, "Cooperative Control Strategy of Energy Storage System and Microsources for Stabilizing the Microgrid during Islanded Operation," *IEEE Transactions on Power Electronics,* vol. 25, pp. 3037-3048, 2010.

[13] M. Fazeli, G.M. Asher, C. Klumpner, L. Yao, "Novel Integration of DFIG-Based Wind Generators Within Microgrids," *IEEE Trans. Energy Conversion,* vol. 26, pp. 840-850, Aug. 2011.

[14] L. Yun Wei and K. Ching-Nan, "An Accurate Power Control Strategy for Power-Electronics-Interfaced Distributed Generation Units Operating in a Low-Voltage Multibus Microgrid," *IEEE Transactions on Power Electronics,* vol. 24, pp. 2977-2988, 2009.

[15] C. Trujillo Rodriguez, D. Velasco de la Fuente, G. Garcera, E. Figueres, and J. A. Guacaneme Moreno. Trujillo Rodriguez, *et al.*, "Reconfigurable Control Scheme for a PV Microinverter Working in Both Grid-Connected and Island Modes," *IEEE Trans. Ind. Electronics,* vol. 60, pp. 1582-1595, Nov. 2013.

[16] L. Gao, R. A. Dougal, S. Liu, and A. P. Lotova. Gao, *et al.*, "Parallel-Connected Solar PV System to Address Partial and Rapidly Fluctuating Shadow Conditions," *IEEE Transactions on Industrial Electronics,* vol. 56, pp. 1548-1556, 2009.

[17] B. HomChaudhuri and M. Kumar, "Market based allocation of power in smart grid," in *Proceedings of the 2011 American Control Conference*, 2011, pp. 3251-3256.

[18] N. S. Wade, P. C. Taylor, P. D. Lang, and P. R. Jones, "Evaluating the benefits of an electrical energy storage system in a future smart grid," *Energy Policy,* vol. 38, pp. 7180-7188, 2010.

[19] R. Majumder, B. Chaudhuri, A. Ghosh, G. Ledwich, and F. Zare, "Improvement of stability and load sharing in an autonomous microgrid using supplementary droop control loop," *IEEE Power and Energy Society General Meeting,* pp. 1-1, Jul. 2010.

[20] X. Wang, F. Blaabjerg, and Z. Chen, "An improved design of virtual output impedance loop for droop-controlled parallel three-phase voltage source inverters," In 2012 IEEE Energy Conversion Congress and Exposition (ECCE), 2012, pp. 2466-2473.

[21] S. Golestan, F. Adabi, H. Rastegar, and A. Roshan, "Load sharing between parallel inverters using effective design of output impedance," In Proc. of the Power Engineering Conference, 2008. AUPEC '08. Australasian Universities, 2008, pp. 1-5.

[22] N. Mohan, T. Undeland, and W. Robbins, *Power Electronics: Converters, Applications and Design*. New Jersey: John Wiley & Sons, Inc., 2003.

[23] A. Keyhani, *Design of Smart Power Grid Renewable Energy Systems*. Hoboken, New Jersey: John Wiley and Sons, 2011.

[24] P. Igic, "Review of Advanced IGBT Compact Models Dedicated to Circuit Simulation," *Facta Universitatis Series: Electronics and Energetics,* vol. 27, pp. 1-12, 2014.

[25] M. N. Marwali, J. Jin-Woo, and A. Keyhani, "Stability Analysis of Load Sharing Control for Distributed Generation Systems," *IEEE Trans. Energy Conversion,* vol. 22, pp. 737-745, Sep. 2007.

[26] M. Trabelsi, L. Ben-Brahim, T. Yokoyama, A. Kawamura, R. Kurosawa, and T. Yoshino, "An improved SVPWM method for multilevel inverters," In Proc. of the 15th International Power Electronics and Motion Control Conference (EPE/PEMC), 2012, pp. LS5c.1-1-LS5c.1-7.

[27] V.F. Pires, J.F. Martins, and C. Hao, "Dual-inverter for grid-connected photovoltaic system: Modeling and sliding mode control," *ScienceDirect: Solar Energy,* vol. 86, pp. 2106-2115, Jul. 2012.

[28] Y. Mohamed and E. F. El-Saadany, "Adaptive Decentralized Droop Controller to Preserve Power Sharing Stability of Paralleled Inverters in Distributed Generation Microgrids," *IEEE Trans. Power Electron.,* vol. 23, pp. 2806-2816, Nov. 2008.

[29] P. H. Divshali, S. H. Hosseinian, and M. Abedi, "A novel multi-stage fuel cost minimization in a VSC-based microgrid considering stability, frequency, and voltage constraints," *IEEE Trans. Power Sys. ,* vol. 28, pp. 931-939, May 2013.

[30] S. Hongtao, Z. Fang, H. Lixiang, Y. Xiaolong, and Z. Dong, "Small-signal stability analysis of a microgrid operating in droop control mode," *IEEE ECCE Asia Downunder (ECCE Asia),* pp. 882-887, Jun. 2013.

[31] M. Antchev and G. Kunov, "Investigation of Three-Phase to Single-Phase Matrix Converter," *Facta Universitatis Series: Electronics and Energetics,* vol. 22, pp. 245-252, 2009.

[32] M. Liserre, R. Teodorescu, and J. Rodriguez, *Grid Converter for Photovoltaic and Wind Power Systems.* Chichester, West Sussex: John Wiley & Sons Inc, 2011.

[33] Z. Grbo, S. Vulkovic, and E. Levi, "A Novel Power Inverter for Switched Reluctance Motor Drives," *Facta Universitatis Series: Electronics and Energetics,* vol. 18, 2005.

[34] J. C. Vasquez, J. M. Guerrero, M. Savaghebi, J. Eloy-Garcia, and R. Teodorescu, "Modeling, Analysis, and Design of Stationary-Reference-Frame Droop-Controlled Parallel Three-Phase Voltage Source Inverters," *IEEE Transactions on Industrial Electronics,* vol. 60, pp. 1271-1280, 2013.

[35] H. Cha, T. K. Vu, and J. E. Kim, "Design and control of Proportional-Resonant controller based Photovoltaic power conditioning system," In *2009 IEEE Energy Conversion Congress and Exposition*, 2009, pp. 2198-2205.

[36] A. Chatterjee and K. B. Mohanty, "Design and analysis of stationary frame PR current controller for performance improvement of grid tied PV inverters," In Proc. of the IEEE 6th India International Conference on Power Electronics (IICPE), 2014, pp. 1-6.

[37] F. de Bosio, L. A. d. S. Ribeiro, M. S. Lima, F. Freijedo, J. M. Guerrero, and M. Pastorelli, "Inner current loop analysis and design based on resonant regulators for isolated microgrids," In Proc. of the IEEE 13th Brazilian Power Electronics Conference and 1st Southern Power Electronics Conference (COBEP/SPEC), 2015, pp. 1-6.

[38] X. Wang, F. Blaabjerg, and Z. Chen, "Autonomous Control of Inverter-Interfaced Distributed Generation Units for Harmonic Current Filtering and Resonance Damping in an Islanded Microgrid," *IEEE Transactions on Industry Applications,* vol. 50, pp. 452-461, 2014.

[39] J. M. Guerrero, V. Luis Garcia de, J. Matas, M. Castilla, and J. Miret, "Output Impedance Design of Parallel-Connected UPS Inverters With Wireless Load-Sharing Control," *IEEE Transactions on Industrial Electronics,* vol. 52, pp. 1126-1135, 2005.

[40] A. Micallef, M. Apap, C. Spiteri-Staines, and J. M. Guerrero, "Performance comparison for virtual impedance techniques used in droop controlled islanded microgrids," In Proc. of theInternational Symposium on Power Electronics, Electrical Drives, Automation and Motion (SPEEDAM), 2016, pp. 695-700.

[41] G. Herong, G. Xiaoqiang, and W.Weiyang, "Accurate power sharing control for inverter-dominated autonomous microgrid," In Proc. of the 7th International Power Electronics and Motion Control Conference (IPEMC), 2012, pp. 368-372.

[42] J.M. Guerrero, J. Matas, V. Luis Garcia de, M. Castilla, and J. Miret, "Decentralized Control for Parallel Operation of Distributed Generation Inverters Using Resistive Output Impedance," *IEEE Trans. Ind. Electron.,* vol. 54, pp. 994-1004, Apr. 2007.

[43] Y. Guan, J. C. Vasquez, J. M. Guerrero, and E. A. A. Coelho, "Small-signal modeling, analysis and testing of parallel three-phase-inverters with a novel autonomous current sharing controller," In Proc. of the IEEE Applied Power Electronics Conference and Exposition (APEC), 2015, pp. 571-578.

[44] Y. Guan, J.C. Vasquez, and J.M. Guerrero, "A simple autonomous current-sharing control strategy for fast dynamic response of parallel inverters in islanded microgrids," In Proc. of the IEEE International Energy Conference (ENERGYCON), 2014, pp. 182-188.

[45] D. Wu, F. Tang, J. M. Guerrero, J. C. Vasquez, G. Chen, and L. Sun, "Autonomous active and reactive power distribution strategy in islanded microgrids," In Proc. of the IEEE Applied Power Electronics Conference and Exposition - APEC 2014, 2014, pp. 2126-2131.